Low Temperature Physics/Fizika Nizkikh Temperatur, 2017, v. 43, No. 9, pp. 1354–1362

Non-isothermal physical and chemical processes in superfluid helium

E.B. Gordon and M.I. Kulish

Institute of Problems of Chemical Physics RAS
Akad. Semenov Ave., Chernogolovka, Moscow region 142432, Russia
E-mail: Gordon@ficp.ac.ru

A.V. Karabulin

National Research Nuclear University MEPhI (*Moscow Engineering Physics Institute*)
31 Kashirskoe Shosse, Moscow 115409, Russia

V.I. Matyushenko

The Branch of Talrose Institute for Energy Problems of Chemical Physics RAS
1 Akad. Semenov Ave., Chernogolovka, Moscow region 142432, Russia

Received December 9, 2016, published online July 25, 2017

Metal atoms and small clusters introduced into superfluid helium (He II) concentrate there in quantized vortices to form (by further coagulation) the thin nanowires. The nanowires' thickness and structure are well predicted by a double-staged mechanism. On the first stage the coagulation of cold particles in the vortex cores leads to melting of their fusion product, which acquires a spherical shape due to surface tension. Then (second stage) provided these particles reach a certain size they do not possess sufficient energy to melt and eventually coalesce into the nanowires. Nevertheless the assumption of melting for such refractory metal as tungsten, especially in He II, which possesses an extremely high thermal conductivity, induces natural skepticism. That is why we decided to register directly the visible thermal emission accompanying metals coagulation in He II. The brightness temperatures of this radiation for the tungsten, molybdenum, and platinum coagulation were found to be noticeably higher than even the metals' melting temperatures. The region of He II that contained suspended metal particles expanded with the velocity of 50 m/s, being close to the Landau velocity, but coagulation took place even more quickly, so that the whole process of nanowire growth is completed at distances about 1.5 mm from the place of metal injection into He II. High rate of coagulation of guest metal particles as well as huge local overheating are associated with them concentrating in quantized vortex cores. The same process should take place not only for metals but for any atoms, molecules and small clusters embedded into He II.

PACS: 67.40.Pm Transport processes, second and other sounds, and thermal counterflow; Kapitza resistance;
67.40.Vs Vortices and turbulence.

Keywords: superfluid helium, coagulation, vortices, heat transfer, radiation cooling.

1. Introduction

Until recently it was believed that superfluid helium (He II) is the simplest homogeneous low-temperature medium for guest particles suspended inside it. It means that the motion of these particles in He II should have a character of simple diffusion, and any physical and chemical processes between them should be strictly isothermal [1,2]. Indeed, such a quantum fluid as liquid helium can be regarded as a continuous medium with spatially averaged characteristics; and in its superfluid state the helium possesses the record high, quantum thermal conductivity, which should eliminate any local overheating [3].

Thus all researchers embedded the guest particles into superfluid helium considered the processes inside He II as strictly isothermal [4–6]. This opinion have been also shared by all the authors, introducing impurity particles into small droplets of superfluid helium [2,7–9].

However, in reality He II is proved to be extremely complex and specific template for the physical and chemi-

cal processes of guest particles. First, it was found [10] that these particles tend to concentrate in the cores of quantized vortices always existing in He II. These vortices are practically one-dimensional objects with a diameter of about 1 Å and a length up to many centimeters [10]. It had recently become clear that due to the collinearity of velocities for particles captured in vortex cores the probability of their collisions there and of subsequent chemical and physical processes is much higher in the vortices than in the bulk [11]. Moreover, the elongation of particles during their coagulation leads to increase of time that the resulting cluster spends in the vortex, and hence, to increase of their local concentration there [11]. This previously unknown rapid process of spatially inhomogeneous condensation should thus produce long thin filaments [12]. The results of experiments with different metals and alloys introduced to bulk He II support this conclusion [13,14]. (As was shown recently, the same behavior demonstrate the metals captured inside large enough superfluid helium droplets) [15,16]. However, it was expected that due to high thermal conductivity of He II the atoms or small clusters will pack tightly, forming either monoatomic chains or nanowires with loose fractal structure. Anyway, the nanowires grown in our experiments fortunately were dense, with almost crystalline packing and «large» diameters of a few nanometers, being close to optimal for many chemical and physical applications [17–19]. Such a behavior was associated with the existence of the limiting heat flux above which the strong turbulence develops in He II. This turbulence disrupts the laminar motion of the normal component, which is responsible for the high heat transfer rate. For the objects larger than micron this effect is known, the threshold heat flow being about 3 W/cm^2 [20]. For very small objects the concentration of vortices is too small to disturb the flow laminarity [21]. In this case, the maximal heat transfer rate W will be determined as the product of the normal component density, the temperature, and the laminar flow velocity restricted by the velocity of second sound in He II, i.e.,

$$W = n_n v_s k_B T, \qquad (1)$$

where $n_n(T)$ is the normal component density, v_s = $= 2\cdot10^3$ cm/s is the velocity of the second sound, and k_B is the Boltzmann constant.

The temperatures of typical experiments on impurity particles introduction in He II are T = 1.6–2.0 K, thus the density of the normal component is about 20–50% of the total liquid helium density, n_n = $(0.4–1.0)\cdot10^{22}$ cm^{-3}. Therefore, the limiting heat flow should be as large as 10^3 W/cm^2 for small particles. For particles of mesoscopic size the heat flow limit is still unknown, but it should be compared with the heat removal rate required, for example, to prevent melting of the merging product of two metal balls of 1 nm diameter each (the clusters of such size are the “bricks” for nanowire growth in the vortex core [17]). This rate estimates as 10^5 W/cm^2 [17]. We believe that even for nanometer metal clusters the limiting heat flow will be also significantly lower than that the above enormously high estimate. (At the same time, in clusters consisting of a few atoms the total energy released during coagulation is not sufficient to form a helium gas cavity insulating heat transfer to the liquid; this problem requires a special consideration which goes beyond the scope of this paper).

Under the above assumptions, the scenario of events taking place presumably above the limiting heat flow is more or less clear: just after the act of coagulation the He II around the merged particles converts to normal He I; it then evaporates to form the sheath filled with low-density helium gas, which reliably insulates the hot core.

The experimental results support our claim, that the coagulation of metal nanoclusters in He II is accompanied by their fusion. Indeed, the dense packing of atoms in the nanowires with “large” (in comparison with vortex core’s thickness) diameters, and the presence of metallic spheres with the perfect shape and atomically smooth surface in the products had been observed [17]. Our model of nanowire formation in He II, which is based on the assumption of adiabatic regime of the coagulation process that leads to cluster melting [17], had been confirmed in several independent studies [22–24]. Nevertheless, we decided primarily to perform a systematic comparison of the diameters of nanowires grown in a low temperature experiments from various metals with those predicted for them by the model [17].

However, by itself, the claim that, for example, tungsten, with its highest melting temperature among all metals, can melt inside the liquid, which cooled down to practically zero absolute temperature and also possesses a record-high thermal conductivity, cannot but cause a certain skepticism from any researcher. Therefore, we have set as a major goal of this work to obtain direct experimental evidence that metal clusters heat up during their coagulation in He II to high, equal to several thousand degrees temperature.

The logic of our experimental study was as follows. According to our model the nanowires are formed by fusing of the spherical clusters with diameters of at least 1 nm. In such clusters the metallic binding already exists [25] and taking into account the high temperatures of clusters the density of free electrons in them must be very high. This means that the intensity of thermal electromagnetic emission should be close for such clusters to that defined by the Planck formula. Liquid helium is optically transparent, and the temperature of the cryostat walls is very low, so that the corresponding thermal radiation is in principle detectable experimentally.

It should be emphasized that the process of nanowires growth in quantized vortices of superfluid helium consists of several non-isothermal stages and which cannot be characterized by a single temperature. Indeed, according to

our mechanism (see [17]), the first stage is the formation of small clusters. At this stage the condensation process is not obviously adiabatic and, moreover, the clusters are still not metals and, hence, there are no free electrons in them. The thermal radiation should be very weak and the first stage should manifest itself as a delay of glowing. The second stage starts when the clusters acquire metallic structure; the clusters are very hot and intensively emit light. The subsequent coagulation diminishes the temperature of the molten cluster and drops eventually its temperature down to melting point. Such clusters could not melt anymore under their collision and they may only fuse together, resulting in nanowire fragments extended along the vortex core. Those fragments then will attach to each other and so on; this stage may be characterized as the third one. Thus, the intense thermal emission is possible only during the second, "bright", stage, and during this stage the clusters of different sizes possess different temperatures. Thus, one cannot speak about a real temperature of this stage, but only judge how the effective temperature is close to the melting point of the metal. The main goal of our study was not in accurate measurements of the temperature, but rather in answering the question, how strong is the local overheating; is it a few or few thousand K? Accordingly, the characteristic coagulation time that we will determine is only the duration of the bright stage.

There is no delayed fluorescence in a metal, and the plasmon excitation by a laser lasts for a time much shorter than a nanosecond [26]. The only source of parasitic light in the microsecond time range is the radiation of plasma excited in the focal spot of the laser. Its contribution must be determined in special experiments.

2. Experimental

Our method for nanowires production in superfluid helium has been described in sufficient detail elsewhere [13]. The experimental setup was assembled on the basis of an optical liquid helium cryostat; the temperature was lowered by pumping the liquid helium vapor down to a pressure of 700 Pa, which corresponds to a temperature of 1.55 K. The atoms and small clusters of metal were introduced into superfluid helium bulk by laser ablation from the surface of submerged in He II targets made of corresponding metals. The pulse-repetition solid state diode-pumped Nd:LSB laser used for ablation had the following characteristics: wavelength $\lambda = 1.064$ μm, pulse energy $E = 0.1$ mJ, pulse duration $\tau = 0.4$ ns, and repetition rate $f = 0$–4000 Hz. Irradiation was carried out through sapphire windows of the cryostat, the laser beam was focused on the target surface to a spot of 50–100 μm in size. The metal particles were captured on the cores of quantized vortices nucleated in the laser focus and then condensate there to form thin nanowires. These nanowires joined together, forming a 3D nanoweb, and fell down to the surface of the standart TEM grids, placed at the cell bottom. Upon warming to room temperature the grids were examined using an electron microscope JEM-2100 (JEOL company).

The design of the apparatus for optical measurements is clear from Fig. 1. Hamamatsu photosensor H11526-110-NN module based on photomultiplier (PMT) equipped with gate function was used to register emission [27]. The sensitive diameter of the photocathode was 8 mm and its spectral sensitivity is shown in [27]. Tektronix TDS 7054 oscilloscope and the custom made gate signal generator also were used.

In integral experiments the photocathode of the photosensor module was placed at 95 mm from the laser focus spot on the surface of metallic targets. In spatially resolved experiments the photo camera objective of 75 mm focal length was arranged so that it provided a double magnification of the image in the vicinity of the laser spot. The PMT, equipped with a 1 mm width slit, could be moved within the plane of this image along the line parallel to laser beam axis. Thus, 0.5 mm spatial resolution was achieved in the time-of-flight measurements.

The gate of PMT was preset using the gate generator at "OFF" ~50 μs before a laser pulse. The signal to set the gate "ON" came simultaneously with the laser pulse from the laser "TRIGGER OUT" and due to the internal delays both in gate generator and photosensor module the PMT was

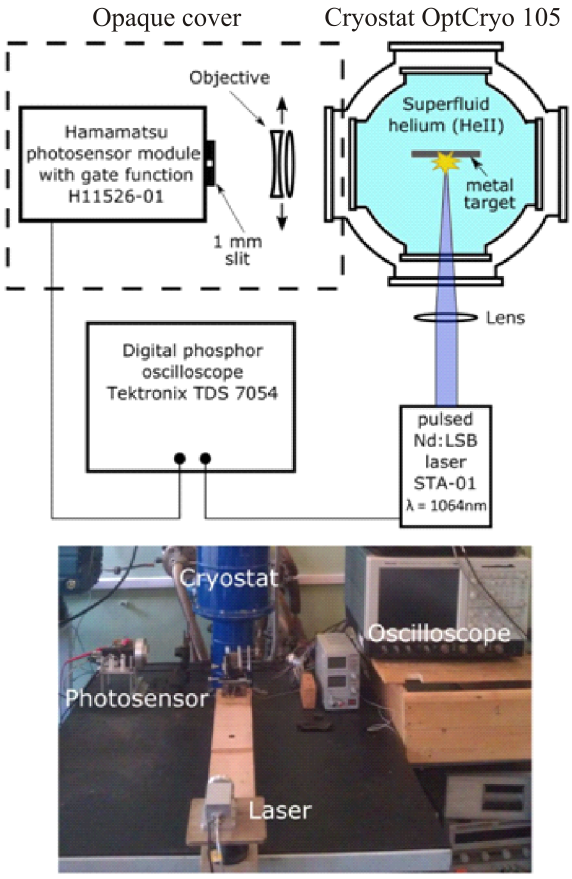

Fig. 1. (Color online) The scheme and photo of the experimental setup for optical measurements.

turned on 180 ns after the laser pulse. In thus way we managed to avoid saturation of the PMT by the large laser signal.

To improve the signal-to-noise ratio, each oscilloscope trace was averaged 128 times. The repetition rates of laser and oscilloscope trigger pulses were 50 Hz. Laser pulses started at zero time of every oscilloscope record.

3. The comparison of diameters of nanowires grown from different metals with the predictions of the model [17]

The morphology of the samples from different metals was quite similar. They represented nanowebs with cell sides of 50-300 nm. The diameter of individual nanowires was practically the same along the whole web, but its value clearly depended on the kind of the metal. It changed from 7-8 nm for fusible indium to 2 nm for refractory tungsten. A simple formula based on thermodynamic and geometric considerations was derived [17]

$$R_{\max} = \frac{Q_b}{\left(C_p T + Q_m\right)} \cdot a\,, \qquad (2)$$

where Q_b is the evaporation heat of the metal; a is the thickness of the monolayer ($a \approx 0.4$ nm); Q_m is the heat of melting, and C_p is the heat capacity of solid metal.

In this paper we compared the diameters of all nanowires grown in our studies [17,28–31] with those predicted as in Eq. (2). It can be seen in Fig. 2, that despite the simplicity of the approach, there is an almost quantitative agreement with all experimental data.

The nanowires made of different metals had, generally speaking, different structure: some of them were single crystals, others were polycrystals or amorphous. However, prior to electron microscope analysis the nanowires were heated up to room temperature and experienced contact with air. Therefore, what structures they had in superfluid helium is unknown. Thin nanowires have proved to possess the low temperature stability [29,30]. In particular, silver nanowires the structure of which was carefully studied [23], when heated to room temperature even changed their topology, breaking up into separate nanoparticles. For us it is important that all nanowires shown in Fig. 2 had close packing, which together with their diameters obeying Eq. (2) constitute the evidence they grew via the stage of molten protoclusters.

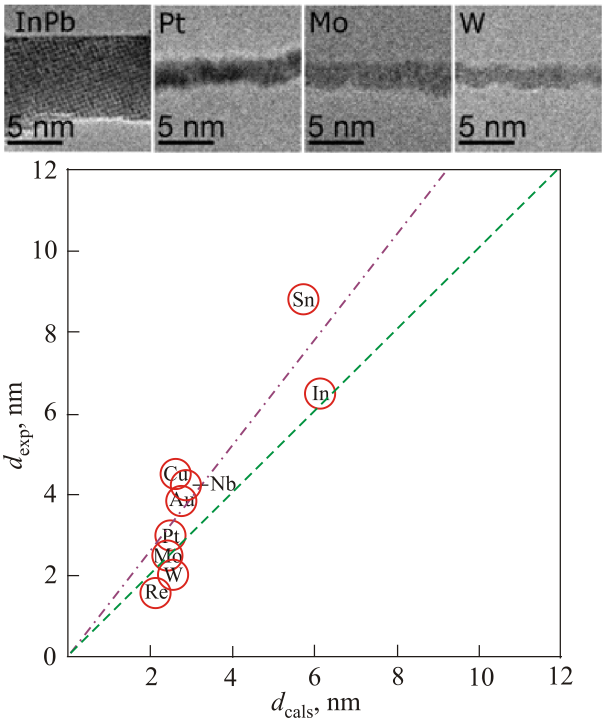

Fig. 2. (Color online) Comparison of the experimental nanowire diameters (d_{exp}) with predictions of Eq. (2). The data for of nanowires made of W, Mo, Pt and InPb alloy are reproduced from Refs. 31–33.

4. Choice of objects

Our goal was to register in an optical range the thermal radiation that accompany the coagulation of metallic particles introduced into superfluid helium by laser ablation from targets of the corresponding metal immersed in He II.

Table 1. Characteristics of the metals studied. T_{melt} and C_p are tabulated values for bulk materials [35]. T_{ad} is the adiabatic temperature of the 1 nm diameter cluster formed by fusion of two cold smaller clusters. D_{clust} is the diameter of the cluster formed by merging of two cold identical spherical clusters, which has a temperature $T = T_{melt}$, $\lambda_{max}(T_{melt})$ and $\lambda_{max}(T_{ad})$ — wavelengths, corresponding to maximal black-body emission for $T = T_{melt}$ and $T = T_{ad}$, correspondingly.

Metal (atomic number)	T_{melt}, K	$\lambda_{max}(T_{melt})$, μm	*T_{ad}, K	$\lambda_{max}(T_{ad})$, μm	Heat capacity, C_p, J/(mol·K)	Latent heat of fusion Q_0, kJ/mol	Full heat of melting $Q = Q_0 + C_p T_{melt}$, kJ/mol	*D_{clust}, nm
In (49)	430	6.44	1900	1.53	26.7	3.24	11.5	4.78
Pt (78)	2041	1.42	3280	0.88	25.9	27.8	52.8	1.97
Mo (42)	2890	1.0	4200	0.69	28	23.93	80.9	1.89
W (74)	3695	0.78	6690	0.43	24.3	35.2	89.8	1.98

Comment: Values marked with * were obtained using the Eq. (5) of Ref. 17.

We wanted to prove that the metal clusters produced by condensation heated up to temperatures of several thousand degrees. That is why we used the photomultiplier sensitive only in visible. The choice of such metals as indium, molybdenum, platinum and tungsten as the objects of study was dictated by the goal of study; their thermal properties are listed in Table 1.

We were guided by the following considerations. According to our scenario, we considered most probable [17] that a nanowire starts to grow when the heat released during two metal clusters fusion becomes insufficient to melt the cluster produced by coagulation. Therefore, at this stage the temperature of clusters should be equal to their melting temperature, which should be lower than the melting point of the bulk metal (T_{melt}). However, for our cluster sizes, the difference is only 10–15% [34] and for a time we will neglect the difference between these two temperatures. As shown in Table 1, the maximum of black-body radiation at T_{melt} for refractory tungsten is close to the red boundary of the PMT sensitivity, so in this case the emission is easy to be registered. In contrast, the maximum black-body radiation at T_{melt} for fusible indium is far beyond the sensitivity range of the PMT, and thus, there is no hope to register an emission during the indium coagulation. Even for molybdenum and especially platinum, which have intermediate melting temperatures, the thermal radiation should be attenuated under registration by orders of magnitude.

However, in the early stages of coagulation the temperature of molten clusters should be much higher than T_{melt}. The temperatures calculated for the adiabatic merging of two spherical clusters with a diameter of 1 nm (which for all metals was less than the diameter of protoclusters) are shown in Table 1. For such clusters the temperatures are really high, so that in the cases of Mo and Pt one could hope to register the thermal radiation during the early stages of coalescence. In the case of indium, in order to have a temperature of 3000 K the clusters had to consist only of a few atoms, and that is too little to display the metal binding: thus, their emissivity should be very low.

Under this logic if the effective temperature of metallic clusters is close to the melting temperature of the respective metal, the large thermal emission signal would be detected only for tungsten. But if the effective temperature of nanoclusters turns out to be significantly higher than T_{melt} the emission for molybdenum and even for platinum would be detectable as well.

5. Optical experiments

Accordingly to the existing understanding of ablation in liquids [36], a gas bubble filled with plasma in laser focus on the surface of target has the characteristic size of a few tenths of mm; the plasma decay products (primarily, atoms and small metal clusters) enter the liquid through the bubble surface. The metal nanoparticles in He II have enough time to cool down before their mutual collisions; otherwise the main products of coagulation would have been micron-size spheres with atomically smooth surface [17]. Ablation efficiencies for all metals under study, as measured via the volume of the crater formed due to laser action, are comparable and can be estimated as 10^{10}–10^{11} atoms per pulse with energy 0.1 mJ.

To distinguish the thermal emission of hot metal nanoclusters in the bulk of He II from the signal registered by PMT it was necessary first of all, to get rid of the scattered laser radiation that could saturate the photomultiplier dynodes by electrons for a long time. The laser pulse duration was 400 ps and the geometric dimensions of the cell could not provide a scattered light delay of more than 1000 ps. It means that the delay of PMT high voltage switch-on of 180 ns allowed us to reliably avoid the effect.

In order to remove the contribution of parasite light from plasma in the laser focus we examined separately the intensity and duration of the gas plasma glow. To do this, the cryostat at the room temperature was filled with helium gas of atmospheric pressure, and the emission of the focal spot followed laser pulses was registered at 45° angle to the plane of the target.

As Fig. 3 shows, the most intensive were plasma glows for indium and tungsten; for molybdenum the intensity was three times lower. This is quite natural, since the intensity of the metal plasma emission depends mainly on the density of energy levels, the probabilities of optical transitions between them, the electron temperature, etc., but in no way it depends on the metal melting temperature. Besides, in all cases the duration of plasma emission did not exceed 1 μs.

The glow that accompanies the condensation of a metal in superfluid helium was registered in the plane parallel to the target. Therefore, the contribution of the emission from the gas bubble near the focal spot was significantly suppressed. Furthermore, as follows from Fig. 3, the glow of the

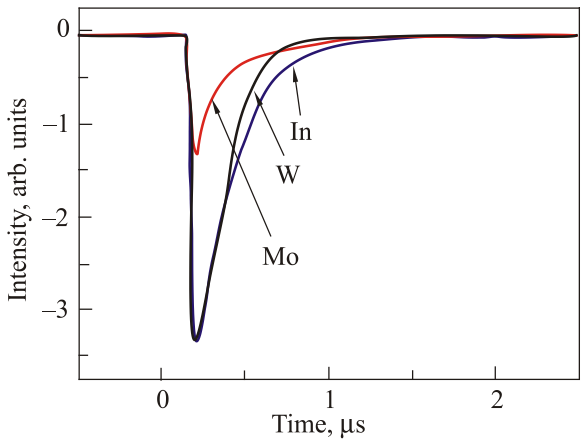

Fig. 3. (Color online) Emission signals from the focal spot for indium, tungsten, and molybdenum. The measurements were performed at 45° relative to the plane of the target in helium gas at room temperature and atmospheric pressure.

plasma gas could not be present in the signal at times longer than 0.5 μs. The dependence of the light intensity in the liquid superfluid helium induced by laser ablation of metal targets is shown in Fig. 4. It is seen that for indium, for which the laser plasma radiation had the same intensity as the tungsten plasma, the emission from the bulk liquid helium is practically absent. This is consistent with our expectations: the estimate made using the spectral PMT sensitivity shows that the intensity of radiation accompanying the indium coagulation should be at least four orders of magnitude lower than that in the case of tungsten. At the same time it served as proof of the weak contribution of the plasma emission from the focal spot to observed signals.

As expected, the emission for tungsten was the highest. However, the emissions for molybdenum and platinum were only a few times less than for refractory tungsten. It is evident that the effective temperatures are even higher than the melting temperature of the respecting metal.

A very important and hard-to-predict feature of the emission from bulk He II is its temporal behavior. It was suggested [6] that the coagulation of impurity particles in the cores of quantized vortices is much faster than in the bulk of superfluid helium, but it was unclear until now, what are the characteristic times of metal coagulation in quantized vortices for typical conditions of experiment. On

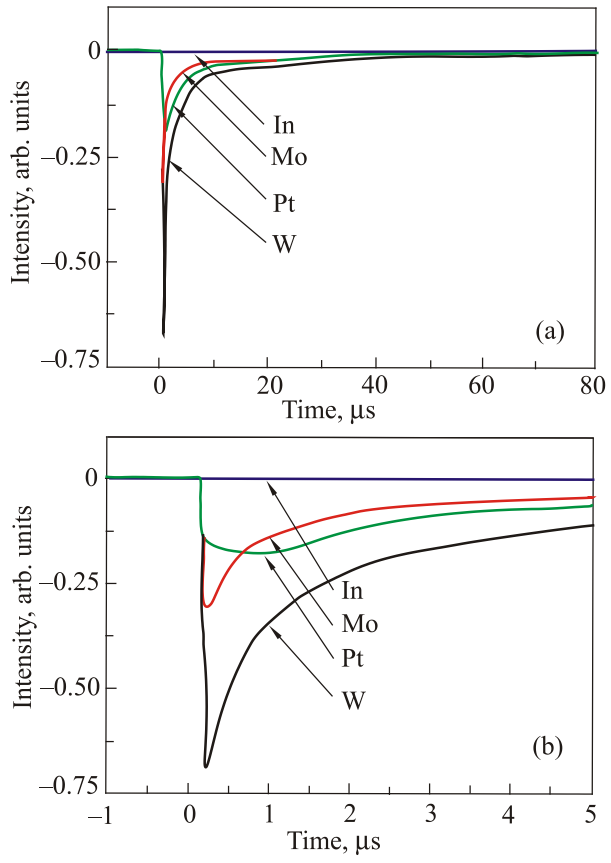

Fig. 4. (Color online) The temporal behavior of the visible emission in bulk He II as induced by laser ablation of In, Mo, Pt and W targets (a). Ditto at a better time resolution (b).

the basis of the observed experimentally independence of nanowires morphology of the laser pulses repetition rate (up to 4 kHz), it was suggested that the whole process of nanowires formation in our experiments takes less than 250 μs [32]. The results of the present study allow us to provide a more definite answer for the question.

As can be seen in Fig. 4, the duration of the "bright" stage of the process, though depending on the type of metal investigated was always much shorter than the above estimate and never exceeded 20 μs. Of course, according to our scenario [9] the "bright" stage of molten spherical clusters growth should be followed by a "dark" stage of their sticking together into nanowires without melting. However, due to the acceleration of the process of metal condensation in quantized vortices with the increase of condensate size, the "dark" stage of the process which corresponds to coalescence of spherical protoclusters, should proceed faster than the "bright" stage of spherical molten cluster growth. On the other hand, as it will be shown below, the whole process of condensation proceeds at the distance less than 1.5 mm from the laser spot, so the geometric factor in collection of the light by the PMT will have no effect on the time profile of the observed signal. However, there are other factors that can change the signal profile, in particular, the metal nanoparticles expansion inside He II, as well as the cooling of hot clusters which may change the spectral composition of the emission.

In order to reveal the role of those factors in the emission, we carried out special experiments. The influence of the metal expansion in superfluid helium on the shape of radiation signals was studied using spatially resolved techniques, namely by moving the photomultiplier equipped with a vertical optical slit 1 mm wide along the doubly magnified image of the coagulation area created by the objective (see Fig. 1). The signals were recorded at the following positions of the optical slit: (i) at the laser spot image, (ii) at a distance of 1.25 and (iii) at a distance of 2.5 mm from it.

From Fig. 5 it is clear, that the expansion of the region of superfluid helium filled with suspended metal is very fast. Its velocities for both W and Mo are close to the Landau velocity (50 m/s) which is the maximal velocity for motion of any guest particles in He II without friction. It is worthwhile to note that the rectangles in Fig. 5 represent the times corresponding to the motion with the Landau velocity in the direction perpendicular to the target surface — for the propagation at some angle to the normal the time of metal appearance at a given distance from the target plane should be longer.

However, the comparison of delayed signal *2* with integrated signal *4* shows that at a distance of 1.25 mm from the focal spot the emission is already quite weak and at a distance of 2.5 mm it disappears completely (see signal *3*). This means that the "hot" stage of coagulation is even shorter than the time needed for the metal to expand and

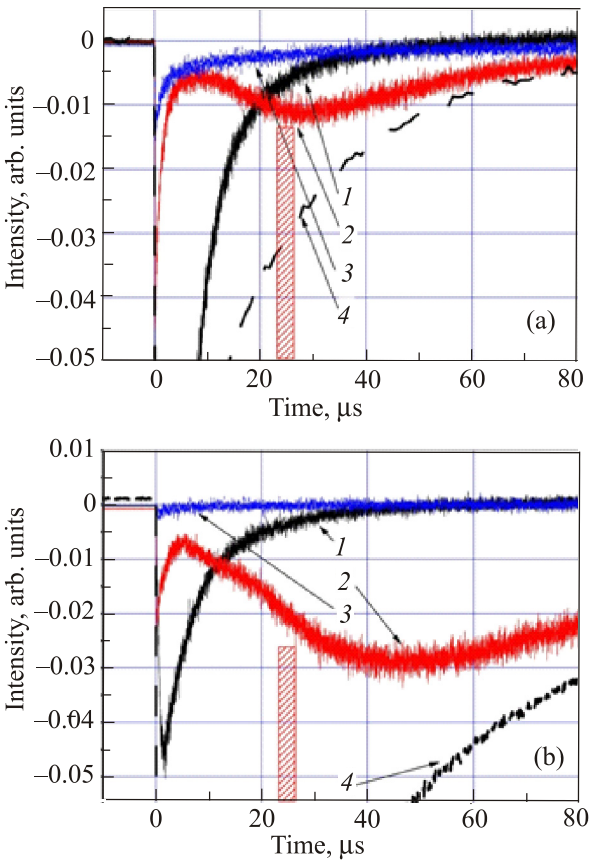

Fig. 5. (Color online) Spatial distribution of the thermal emission of tungsten (a) and molybdenum (b) in superfluid helium. The curves corresponded to three distances from laser focus: 0 (*1*), 1.25 (*2*), and 2.5 mm (*3*). The rectangles mark the moment of arrival at observation point 1.25 mm of the flat front moving with Landau velocity, V_L = 50 m/s. Curves *4* are the integrated emission signals as registered for the similar conditions without optical slit.

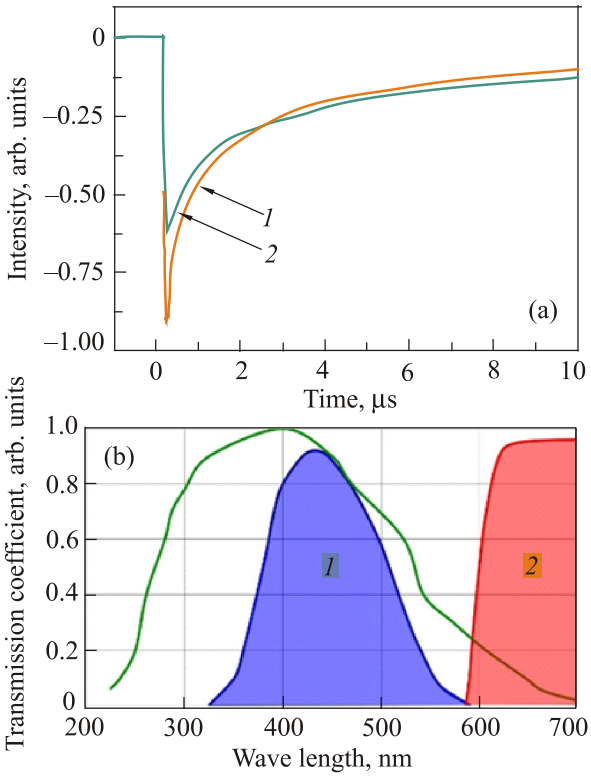

Fig. 6. (Color online) The thermal emission accompanying the tungsten coagulation as registered through the "blue" (*1*) and "red" (*2*) filters (a); transmission spectra through "blue" (1) and "red" (2) filters; the normalized spectral sensitivity of the PMT cathode presented in Figure as well (green curve) (b).

the whole process of metal condensation in superfluid helium occurs in vicinity of the place of ablation.

Methodologically, it is a very important result. It shows that the intensity of the laser ablation, which we used for nanowires synthesis, leads to an initial concentration of the metal embedded into the He II so high that the whole coagulation process in the vortices occurs very close to the surface of gas bubble existed in laser focus. This, of course, does not promote formation of high-quality and long nanowires.

The emission spectra were not studied in our experiments. Yet, in order to reveal how strong are the temporal changes of the radiation spectra we used the broadband glass filters, "blue" SZS20 and "red" KS10 (their transmission spectra together with the spectral sensitivity of PMT photocathode are shown in Fig. 6). Taking into account the spectral efficiency of the cathode, one can consider that the first filter spans the 380–450 nm spectral range while the second one registers the radiation in the 600-650 nm region. Figure 6(a) shows the time dependence of the intensity of the emission induced by tungsten coalescence as registered using the "blue" (*1*) and "red" (*2*) filters. Both amplitudes are of close, but since the energy width of the "red" filter is four times smaller than that of the "blue" one and the PMT efficiency in the "red" is four times lower than in the "blue", we conclude that over 90% of the energy is concentrated in the red wing of the emission spectrum. This is consistent with our approximation of tungsten protoclusters as blackbody with a temperature below 4000 K. The comparison of curves *1* and *2* shows clearly that at short times the blue part of the spectrum is more intensive than later. This is obvious evidence that the emitter cools down during the emission, yet, as it follows from our estimates, this effect is rather small.

But if so, the characteristic times of radiation signals presented in Fig. 4 reflect mainly the kinetics of metal clusters coagulation in superfluid helium. To estimate the rate of such coagulation it makes sense first of all to use a simplified representation of the coagulation as a simple bimolecular coalescence of two identical clusters which can be described by the kinetic equation:

$$\frac{dn}{dt} = -kn^2 \qquad (3)$$

giving the hyperbolic temporal dependence of the reagent concentration

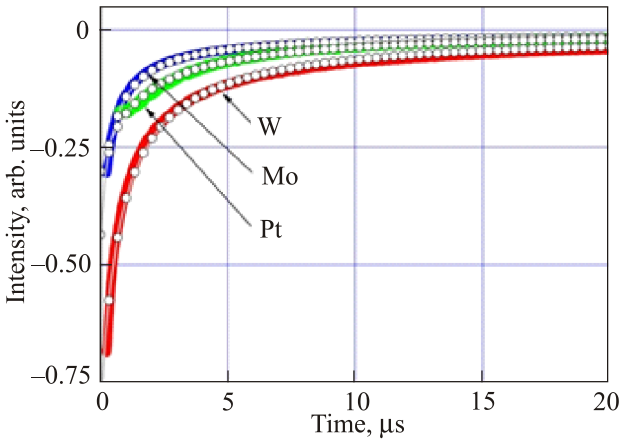

Fig. 7. (Color online) The approximation of the thermal emissions temporary dependencies by the hyperbolic law for tungsten, platinum and molybdenum. Solid curves are an experimental results, open circles represent hyperbolic dependencies.

$$n = \frac{n_0}{1 + kn_0 t} + C \tag{4}$$

The coefficient C is responsible for the background due to scattered light of the room illumination. As seen in Fig. 7, for all metals emission intensity decrease fits well the hyperbolic dependence characteristic for the recombination.

For molybdenum and especially for platinum there are some deviations at short times. We expected such effects as a manifestation of the fact that very small clusters that appear at the first stage of coagulation have a non-metallic binding. In this case they do not contain free electrons and their thermal emission should be much weaker than it follows from the Planck formula for the blackbody.

The coefficients corresponding to the extrapolations shown in Fig. 7 have the following meanings: n_0 is the initial concentration of the atoms, and k_0 is basically the rate constant of the bimolecular reaction of two clusters sticking together. Since the reagents captured at the vortex can move only along the its core the reaction should be considered as one-dimensional and the rate constant for different metals should represent the ratio of the velocities of their motion inside the vortex. From Fig. 7 it follows that the "rate constant" ratios k_{Mo} (42) : k_W (74) : k_{Pt} (78) = = 4.9 : 3.7 : 2.3 (atomic weights are in brackets) do not contradict this interpretation: the lighter the atom, the faster its motion along the core of the vortex.

Because of the hyperbolic dependence on time there is no concept of characteristic time for coagulation process but, as shown in Fig. 7, under conditions of our experiments the process lasts about 2 μs.

6. Conclusions

The entire body of data related to the production of nanowires by condensation of different metals inside superfluid helium demonstrates, that the structure of nanowires (qualitatively) and their diameters (quantitatively) confirm the scenario of metal coagulation in quantized vortices in He II as proposed in Ref. 17. According to this scenario, during the initial "hot" stage the small metal clusters, even if they were previously cooled to low temperature, fuse to larger clusters and simultaneously heat above their melting temperatures. Only starting from the clusters with diameter exceeded its limiting value, determined by thermo-chemical properties of the metal, they stick together into nanowires.

According to this scenario, the nanoparticles heated above their melting temperature should exist during the initial stages of metal condensation in He II. Provided they grow up to nanometer size such clusters acquire metallic binding and thus contain a lot of free electrons (especially when they are heated up to high temperatures). For that reason they should intensively emit photons in IR, and even in visible spectrum. This radiation has been experimentally detected in the bulk He II during the condensation of tungsten, molybdenum, and platinum. The spectral region of this emission is the argument that it belongs to clusters heated up to at least the metal melting point. At the same time, the fusible indium, whose laser plasma emits in the visible not less efficiently than other metals under study, does not demonstrate any visible radiation during coagulation; this confirms the thermal nature of the emission.

The surprising fact of refractory metal melting in He II is the consequence of the specific character of heat transfer in superfluid helium. He II possesses enormously high thermal conductivity but only up to a rather low value of heat flow. Above this limit the heat flow becomes suppressed due to the development of turbulence. Superfluid helium then converts to the normal fluid state, and then evaporates to form a heat insulating envelope filled with low-pressure helium gas.

The kinetics of thermal radiation decay, as registered in our study and explained above is the first indication of abnormally high rate of coagulation of impurities via their one-dimensional motion towards each other along quantized vortices. It turns out that with the actual metal concentrations created inside He II in our experiments, the entire condensation process takes place very close to the surface of the gas plasma bubble in the laser focus, the turbulence being quite strong.

As shown in this study, the expansion of the metal inside liquid helium is surprisingly fast, with the velocity close to Landau velocity (despite the fact that at temperature of our experiments, T = 1.7 K, the fraction of the normal, viscous component is still rather high). But even this large rate is insufficient to compete with process of coagulation.

The important conclusions of this work are.

The existence of huge local overheating is the result of the unique properties of superfluid helium, and it is expected not only for metals. Similar effects could be observable not only in the bulk liquid helium, but also in cold helium droplets [2,7–9,15,16]. If a liquid helium droplet contains guest

atoms, molecules or, especially, clusters, the overheating during their chemical or photochemical processes could result in the appearance of gas cavity in the droplet. Indeed, the high temperature of metal clusters in He II exists, as follows from our results, for a time of about 10^{-6} s, which is a few orders of magnitude longer than the time of sound wave propagation in liquid helium from the center of droplet to its surface. Because of the zero pressure around a droplet the gas cavity is expected to appreciably expand during that time. Besides, existence of a radiative (without helium atoms evaporation) channel of cluster cooling can entail to underestimation of the final droplet size.

And finally, the local overheating should occur not only in the case of chemical reactions between the particles embedded into He II, but also during coalescence of chemically inert particles. Indeed Van der Waals forces are weaker than chemical ones only by about 30 times. It means that in this case local overheatings of 30–100 K, which is significant at cryogenic temperatures, can be observed.

Thus, the existence of huge local overheatings kills any promises of producing under the special conditions of superfluid helium any entity made of exotic chemical compounds. However, it simultaneously guaranties a hope to use He II for synthesizing unique nanomaterials, the exotic properties and high possible cost of which justify application of expensive and small-scale method of their production.

Acknowledgments

The authors are grateful to E.V. Dyatlova, A.S. Gordienko and M.E. Stepanov for participating in the experiments.

This work was financially supported by Russian Science Foundation (grant No. 14-13-00574).

1. K.K. Lehmann and G. Scoles, *Science* **279**, 2065 (1998).
2. J.P. Toennies and A.F. Vilesov, *Angew. Chem. Int. Ed.* **43**, 2622 (2004).
3. R.J. Donnelly, *Quantized Vortices in Helium* II, Cambridge University Press, Cambridge (1991).
4. E.B. Gordon, L.P. Mezhov-Deglin, and O.F. Pugachev, *JETP Lett*. **19**, 103 (1974).
5. E.B. Gordon, *Fiz. Nizk. Temp*. **30**, 1009 (2004) [*Low Temp. Phys.* **30**, 756 (2004)].
6. V.V. Khmelenko, E.P. Bernard, S.A. Vasiliev, and D.M. Lee, *Russ. Chem. Rev*. **76**, 1107 (2007).
7. A. Bartelt, J.D. Close, F. Federmann, N. Quaas, and J.P. Toennies, *Phys. Rev. Lett.* **77**, 3525 (1996).
8. J. Tiggesbäumker and F. Stienkemeier, *Phys. Chem. Chem. Phys*. **9**, 4748 (2007).
9. C. Callegari and W.E. Ernst, *Handbook of High Resolution Spectroscopy*, John Wiley & Sons, Chichester (2011).
10. G.A. Williams and R.E. Packard, *Phys. Rev. Lett*. **33**, 280 (1974).
11. E.B. Gordon, R. Nishida, R. Nomura, and Y. Okuda, *JETP Lett*. **85**, 581 (2007).
12. E.B. Gordon and Y. Okuda, *Fiz. Nizk. Temp*. **35**, 278 (2009) [*Low Temp. Phys*. **35**, 209 (2009)].
13. E.B. Gordon, A.V. Karabulin, V.I. Matyushenko, V.D. Sizov, and I.I. Khodos, *Fiz. Nizk. Temp*. **36**, 740 (2010) [*Low Temp. Phys.* **36**, 590 (2010)].
14. P. Moroshkin, V. Lebedev, B. Grobety, C. Neururer, E.B. Gordon, and A.Weis, *EPL* **90**, 34002 (2010).
15. E. Latimer, D. Spence, C. Feng, A. Boatwright, A.M. Ellis, and S.F. Yang, *Nano Lett*. **14**, 2902 (2014).
16. P. Thaler, A. Volk, F. Lackner, J. Steurer, D. Knez, W. Grogger, F. Hofer, and W.E. Ernst, *Phys. Rev. B* **90**, 155442 (2014).
17. E.B. Gordon, A.V. Karabulin, V.I. Matyushenko, V.D. Sizov, and I.I. Khodos, *JETP* **112**, 1061 (2011).
18. E.B. Gordon, A.V. Karabulin, V.I. Matyushenko, V.D. Sizov, and I.I. Khodos, *Appl. Phys. Lett.* **101**, 052605 (2012).
19. E.B. Gordon, A.V. Karabulin, V.I. Matyushenko, T.N. Rostovshchikova, S.A. Nikolaev, E.S. Lokteva, and E.V. Golubina, *Gold Bulletin* **48**, 119 (2015).
20. J. Fang, A.E. Dementyev, J. Tempere, and I.F. Silvera, *Rev. Sci. Instrum* **80**, 901 (2009).
21. S. K. Nemirovskii, *Phys. Rep*. **524**, 85 (2013).
22. D. Spence, E. Latimer, C. Feng, A. Boatwrigh, A.M. Ellis, and S. Yang, *Phys. Chem. Chem. Phys*. **16**, 6903 (2014).
23. A. Volk, D. Knez, P. Thaler, A.W. Hauser, W. Grogger, F. Hofer, and W.E. Ernst, *Phys. Chem. Chem. Phys*. **17**, 24570 (2015).
24. E.Fonda, K.R. Sreenivasan, and D.P. Lathrop, *Rev. Sci. Instrum*. **8**, 025106 (2016).
25. L.J. Jongh, *Physics and Chemistry of Metal Cluster Compounds: Model Systems for Small Metal Particles*, Springer, Netherlands (1994).
26. J. Passig, R. Irsig, N.X. Truong, T. Fennel, J. Tiggesbaumker, and K. H. Meiwes-Broer, *New J. Phys*. **14**, 085020 (2012).
27. http://www.hamamatsu.com/jp/en/H11526–110.html.
28. E.B. Gordon, A.V. Karabulin, V.I. Matyushenko, V.D. Sizov, and I.I. Khodos, *J. Low Temp. Phys*. **172**, 94 (2013).
29. E.B. Gordon, A.V. Karabulin, V.I. Matyushenko, V.D. Sizov, and I.I. Khodos, *Phys. Chem. Chem. Phys*. **16**, 25229 (2014).
30. E.B. Gordon, A.V. Karabulin, V.I. Matyushenko, and I.I. Khodos, *J. Phys. Chem. A* **119**, 2940 (2015).
31. E.B. Gordon, A.V. Karabulin, A.A. Morozov, V.I. Matyushenko, V.D. Sizov, and I.I. Khodos, *J. Phys. Chem. Lett*. **5**, 1072 (2014).
32. E.B. Gordon, A.V. Karabulin, V.I. Matyushenko, V.D. Sizov, and I.I. Khodos, *Laser Phys. Lett*. **12**, 096002 (2015).
33. E.B. Gordon, A.V. Bezryadin, A.V. Karabulin, V.I. Matyushenko, and I.I. Khodos, *Physica C* **516**, 44 (2015).
34. W.H. Qi, *Physica B* **368**, 46 (2005).
35. *Tables of Physical Quantities: A Reference Book*, I.K. Kikoin (ed.), Atomizdat, Moscow (1976) [in Russian].
36. G.W. Yang, *Prog. Mater. Sci*. **52**, 648 (2006).